https://doi.org/10.5281/zenodo.17173606 Ife Journal of Technology, Vol. 30(1), 2025

Optimal Time and Power Allocation for Throughput Fairness in RF-Energy Harvesting Cognitive Radio Networks

Enoruwa Obayiuwana[1], Akinbode A. Olawole[1], Oluwafemi Ipinnimo[2], Folorunso C. Oluwaseyi[2]
[1]Department of Electronic and Electrical Engineering, Obafemi Awolowo University, Ile-Ife, Nigeria.
[2]Department of Systems Engineering, University of Lagos, Lagos, Nigeria.

ABSTRACT

In this study, we addressed the optimization problem of fair network resource allocation in the context of cognitive radio network radio frequency energy harvesting (CRN-RF-EH) networks to ensure unbiased distribution of throughput capacity among users in the system. To achieve this goal, we formulated a non-convex optimization problem, specifically a max-min resource allocation problem. To make it more manageable, we transformed this non-convex problem into a convex optimization one by introducing auxiliary variables. We demonstrated that the transformed optimization problem is concave. We maximize the CRN-RF-EH worst-case user throughput capacity through the proposed joint optimal time and power allocation (JOTPA) scheme under the prevailing CRN-RF-EH constraints. Through simulation results, we consistently observed superior performance of our proposed solution compared to the conventional biased-randomized time optimal power allocation (BRTOPA) scheme. It is important to note that our analysis of the radio resource allocation fairness in CRN-RF-EH assumes perfect channel state information (CSI) among all users. In future research, exploring the impact of uncertainty arising from imperfect CSI among users in CRN-RF-EH would be an interesting direction.

KEYWORDS

Cognitive Radio Networks
Energy Harvesting
Fairness
Optimization
Radio Resource Allocation

1. INTRODUCTION

The rapid expansion of wireless communication networks, driven by increasing demand for connectivity and diverse applications, has heightened global energy consumption (Wang & Lee, 2022). For the next-generational wireless networks (NGWNs) to be sustainable, various green energy sources, such as solar energy, wind energy, geothermal energy, radio frequency (RF) energy, etc. are actively being proposed as alternatives to fossil fuel energy source replacements for these wireless communication networks (Gholikhani et al., 2020). The RF energy harvester can convert a wide spectrum of radio frequency energy into usable electrical energy. The RF energy harvesting networks can be implemented using two different architectures, namely: the harvest-use architecture and harvest-store-use architecture. The energy harvested in the harvest-use model is used directly by the communication device without any form of energy storage. In the harvest-store-use architecture, the energy harvested is stored in batteries or super-capacitors, this stored harvested energy is made available to the communication node and used when it is required for its functional applications. The operational protocols of RF harvesting networks are generally time-slotted. For a complete communication time frame, a time slot is given for wireless power transfer (WPT) (Zhang et al., 2019) and wireless information transfer (WIT), however, when both WET and WIT take place concurrently this is referred to as Simultaneous wireless information and power transfer (SWIPT) (Wu et al., 2022).

Cognitive radio (CR) technology is another major disruptive technology proposed for NGWNs. Cognitive radio networks (CRN) have a huge potential to improve poor radio spectra utilization and address the radio spectra scarcity challenges that are currently faced in the wireless communications industry. The CRN is a secondary user (SU) networks that seek to utilize the licensed radio spectrum of the primary users (PU) network without causing harmful interference to the PUs in the primary network. Three different architectures have been exploited to achieve the radio spectrum access goals of CRN. These are the overlay, interweave and underlay spectra access models (Zakariya et al., 2020). The underlay spectrum access model is regarded as the most efficient in terms of spectra utilization (Zakariya et al., 2020).

The integration of CR and RF-EH technologies provides tremendous capability of access to "free" spectra and energy. These capabilities have proved to be of interest to both wireless communication researchers in academia and the industry (Singh et al., 2020). The underlay spectrum access provides the best spectrum access paradigm for CRN-RF-EH. The SU in the underlay spectrum access mode in the CRN-RF-EH will utilize all its harvested energy for its sole radio transmission purpose. The SU is not engaged in spending any fraction of its harvested RF energy on PUs spectrum sensing in the case of inter-weave spectrum access mode or cooperative relaying for the PU, as in the case of the overlay spectrum access mode. Hence, a lot of research interests have developed for the underlay CRN-RF-EH.

In low-powered and spectra-constrained wireless communication networks, resource starvation for wireless communication nodes located at the far-edge of the communication network can readily occur. Ignoring the radio resource allocation fairness of these nodes can result in significantly reduced throughput capacity for some cell-edge user nodes with poor channel conditions. Various resource allocation strategies such as max-min fairness, round-robin fairness, harmonic mean rate fairness and proportional fairness exist in the literature (Liu & Zhang, 2020). A proportional fairness allocation strategy can possibly deny data transmission to some users in the CRN-RF-EH with high interfering channel gains to the PU or inappropriate channel gain conditions. This wireless network scenario can make the proportional fair allocation strategy not very attractive to employ in this CRN-RF-EH. Hence, we consider another fairness criterion: max-min fairness. This allocates to each user in the CRN-RF-EH a reasonable practical capacity rate. The max-min fairness allocation usually provides the highest resource allocation and usage to the user who is most resource-starved (Lee & Shin, 2023). Our goal in this paper is to jointly optimize the allocated transmit time and allocated transmission power in the CRN-RF-EH so that, under the constraints of energy causality, communication frame duration, maximum power, and allowable interference of the PU networks, the worst-case user capacity of the network is maximized.

Corresponding Author: E. Obayiuwana (*enoruwa.obayiuwana@alumni.uct.ac.za*)
The editor responsible for coordinating the review of this article and approving its publication was *K.P. Ayodele.*
P-ISSN: 1115-9782 **e-ISSN:**

This paper tackles the challenge of radio resource allocation fairness in a multi-user that specifically allows multi-user in the CRN-RF-EH to have uniform access to the CRN-RF-EH networks' transmission resources, irrespective of the multi-user's wireless radio environment or conditions. The paper fills this gap by presenting and exploring the max-min optimization framework for multi-user in a low energy constrained CRN-RF-EH network, while optimizing the transmission time and power of the nodes in the CRN-RF-EH Network.

The radio resource management (RRM) function is a core aspect of wireless communication networks. Nevertheless, the investigation into the resource allocation fairness issues in CRN-EF-EH has received little attention. This work investigates the joint transmission time and transmits power allocation strategy in CRN-RF-EH with the aim to maximize the worst-case user' capacity, such that the user's starvation does not occur and the interference constraint threshold of the primary user in the primary networks is not violated. This is especially crucial for the wireless communication networks with finite energy capacity in a low-powered wireless communication network where resource starvation can readily occur. The max-min fairness optimization approach helps to solve the problem of providing the same maximum QoS for the individual user irrespective of their challenge propagation environment, thus this optimizes for the weakest user network throughput. Maxi-min optimization ensures that there is no resource starvation for the network resource user (Raeisi-Varzaneh et al, 2023). In this paper, the worst-case user capacity maximization investigation is formulated as max-min optimization problem OP1 through the joint optimization of the transmit power and transmit time. The problem **OP1** is observed to be a non-convex optimization problem. First, we introduce a slack variable and a new auxiliary variable, we transformed OP1 into an optimization problem **OP2**. Next, we observed that due to the coupled variables in some of the constraints of **OP2**, an intermediate variable is introduced to transform **OP2** to a standard convex optimization problem, OP3. For the maximization of the worst-case user capacity, a joint optimal time and power allocation (JOTPA) scheme is proposed. We showed that the global optimal solution exists since the optimization problem as formulated is a standard convex problem. Thus, the problem can be solved efficiently by using any standard convex optimization technique. Furthermore, using the commercial CONOPT solver package implemented in the MATLAB environment, the standard convex optimization problem is solved to obtain the optimal values of the decision variables, transit time and power allocation for the worst-case user capacity maximization. The results obtained for the numerical simulations of the JOTPA strategy are compared with the baseline biased-randomized time optimal power allocation (BRTOPA) scheme.

The rest of the paper is organized as follows: Section 2 provides a related literature review on CRN-RF-EH. Section 3 introduces the system network framework for the proposed joint time and power resources allocation optimization problem with fairness considerations of the CRN-RF-EH. In Section 4, the mathematical model of the problem is formulated and then solved using CONOPT optimization package. Furthermore, Section 6 presents and discusses the performance evaluation of the proposed scheme. Finally, Section 7 concludes the paper.

2. RELATED WORKS

Xu et al. (2018) investigated the energy maximization problem for multiple SUs in multi-channel energy harvesting networks through the joint allocation of channel and transmission power for the SUs nodes. The investigated energy maximization problem formulation led to a non-convex mixed-integer non-linear fractional programming (MINLFP) problem. To obtain the solution to the non-convex energy efficient optimization problem, the binary constraint of channel selection is relaxed and the fractional objective function is transformed into multiple objective functions with the help of a parametric variable and solved using the Dinkelbach method. Finally, the numerical results obtained are compared to the reference equal power allocation scheme. The proposed algorithm significantly improves the energy efficiency of the CRN-RF-EH compared to the equal power allocation algorithm. While this work tackles the issue of network throughput capacity maximization, however the network resource allocation fairness is not addressed.

Hu et al. (2017), in their work, investigated the optimal max-min fairness resource allocation for wideband cognitive radio with energy harvesting capability. The system model for the wide-band network is made of severalPUs, a single cognitive base station (CBS) and several SUs with the CBS operating in the simultaneous wireless information and power transfer (SWIPT) mode. The CBS first senses the $PU's$ spectrum to ascertain the status of the $PU's$ channels. When the $PU's$ channel is vacant, the CBS engages in SWIPT with the SUs and energy harvesting Receivers (EHRs). To address the resource allocation issues of the narrow-band channel allocations to the SUs, the worst-case user capacity maximization was proposed, but the wide-band sensing of the PUs spectrum by the single CBS node may limit the performance of the network.

Jiang et al. (2017) developed a cooperative sensing framework that jointly optimizes the spectrum sensing time and energy harvesting time to maximize the spectrum access probability for the CRN-RF-EH. The sum throughput maximization for multiple access cognitive radio networks with cooperative spectrum sensing and energy harvesting is investigated in (Biswas et al., 2019). However, cognitive radio cooperative sensing can incur a variety of cooperation overheads. This may deteriorate the overall performance of the CRN-RF-EH.

Cheng et al. (2017) considered proportional fairness in cognitive wireless-powered communication networks (CWPCN). The CWPCN accesses the licensed spectrum based on the underlay spectrum sharing framework. The CWPCN is based on the time division multiple access (TDMA) transmission scheme and harvest-then-transmit protocol. The users far away from the hybrid access point (HAP) achieve low throughput, as they suffer from both low harvested energy and high energy consumption for transmission. Hence, this unfairness issue is referred to as the doubly near-far phenomenon. To address this problem in (Cheng et al., 2017), the authors adopted the bandwidth utility maximization framework, based on proportional fairness. Simulation results showed that the proposed scheme outperformed the sum capacity scheme in terms of fairness metric and similarly provided a trade-off between fairness and throughput.

Kalamkar et al. (2016) present an overlay cognitive radio network, where the cognitive nodes are powered by a dedicated RF energy source from the HAP. To maximize the sum throughput capacity of the secondary network in (Kalamkar et al., 2016), the sum throughput optimal resource allocation (STORA) scheme that jointly selects the optimal SU for cooperative relaying, energy harvesting time and transmission power allocation is developed. However, as the STORA scheme prioritizes sum throughput, the STORA scheme may neglect SUs with poor channel gains, resulting in poor fairness performance. To address this challenge, the authors considered three resource allocation schemes: equal time allocation (ETA), minimum throughput maximization (MTM) and proportional time allocation. Simulation results demonstrate a trade-off between sum throughput and fairness.

3. SYSTEM MODEL

We consider cognitive radio networks with radio frequency energy harvesting (CRN-RF-EH) capabilities. The CRN-RF-EH network is based on the undelay spectrum access and TDMA model. Our model design is based on the justification that underlay spectrum access architecture is not plagued with spectrum sensing overhead, high latency for secondary users and the requirement explicit cooperation primary users. Furthermore, the TDMA in our model justifiably maximizes all usable bandwidth with no need bandwidth wastage on guard bands and reduces the complexity of frequency assignment in wireless cellular communication networks. These are widely adopted wireless communication networks industry standards (Cheng et al., 2017),

hence the motivation of the adoption of these models in this paper. A multi-user CRN-RF-EH with an underlay spectrum access architecture is considered. The CRN-RF-EH consists of multi-user equipped energy harvesting modules as shown in Figure. 1 and Figure. 2. The primary user networks consist of a single PT and PR . The PT is constantly transmitting within the primary user networks. The CRN-RF-EH has the side information of the maximum interference threshold of the primary networks. The primary network has the licensed spectrum usage right. However, it can allow the secondary network to access the spectrum using the underlay access mode. Thus, the network performance of the primary networks is not degraded by transmission activities of the secondary networks. The secondary user network consists of i^{th} transmitter and i^{th} receiver, where $i^{th} \in (1,2,3,\cdots,M-1,M)$. Each SU node is equipped with a single antenna. Through underlay spectrum access and RF energy harvesting, the secondary users, have access to both "free" spectrum and "free" energy for their transmissions.

The transmitting SU operates on harvest-store-use. SUs are equipped with super-capacitors for harvested energy storage. A complete communication frame duration,T_F , of the CRN-RF-EH is divided into M slots, where M is the number of secondary users in the CRN-RF-EH. Each complete communication slot duration T is divided into two sub-slots. The sub-slot at the beginning of each communication slot duration is the SU energy harvesting time slot, while the remaining or second sub-slot of the communication slot duration is the SU information transmission time slot. The SUs cannot transmit their information while they are harvesting energy from the PU transmitter and similarly the SUs cannot harvest energy from the PU transmitter, when they are transmitting their information. However, SUs located far from the PT will experience higher distance-dependent path-loss attenuation than SUs located near the PT. This might lead to unfairness in resource access, whereby distant cell-edge users from the PT not only have less chance to harvest energy but may also have insufficient energy for their transmission when compared to SUs which are relatively closer to the PT. Let the i^{th} user be denoted by U^i, while the ith transmitter and the i^{th} receiver are denoted by U_{ST}^i and U_{SR}^i, respectively. The energy harvesting channel gain between the PT and the U_{ST}^i is denoted as $a_{PT,ST}^i$, similarly, the interference channel gain between the U_{ST}^i and the $U_{SR}^i$is denoted by $b_{PT,SR}^i$. The noises at both PR and U_{SR}^i are considered to be both independent and identically distributed (i.i.d.) circularly symmetric complex Gaussian with zero mean and variance of σ^2. The network system models a dense urban city environment where there is no line of sight (NLOS) path. Thus, all the channel links in the model experience both large-scale fading and small-scale fading. The U_{ST}^i node is powered by the harvested energy. The SU^i is a single antenna-equipped node that cannot transmit and receive simultaneously; thus, it operates in half-duplex mode. The CRN-RFEH system model adopts the harvest-then-transmit protocol. In the CRN-RF-EH, the frame duration of T_F is divided into M slots. A slot has a duration length T. The i^{th} user is assigned to the slot, $S(i)$. Each user's slot duration, T is divided into two sub-slots. This is the energy harvesting time sub-slot and the information transfer time sub-slot. At the beginning of the $S(i)$ slot, the U_{ST}^i will have to harvest its energy from $PT's$ RF signal before transmitting its data. This is referred to as the energy harvesting slot. The harvested energy can temporarily be stored in a super-capacitor, until the U_{ST}^i is ready to transmit its information or data to the U_{SR}^i. The super-capacitor is assumed to be fast charging and has infinite recharge cycles. In the CRN-RF-EH, we adopt a time division multiple access (TDMA) scheme, where each time block T consists of two phases. The SUs transmit their information at orthogonal time slots. The energy harvested in the harvesting slot is consumed (Sharma, P. & Singh, A. K, (2023), at the end of each user's network communication slot duration. Thus, energy harvested in a given slot cannot be used in another slot. The fame duration, T_F and slot structures are shown in Figure. 3.

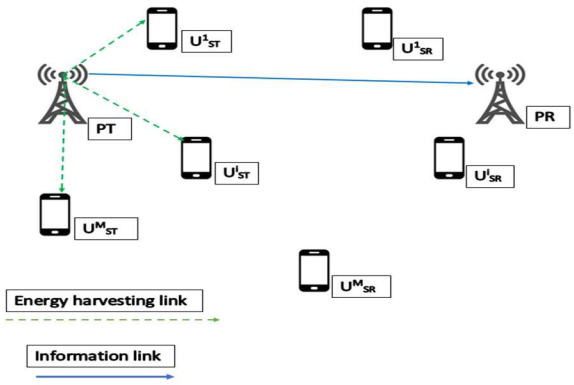

Figure. 1: Energy harvesting

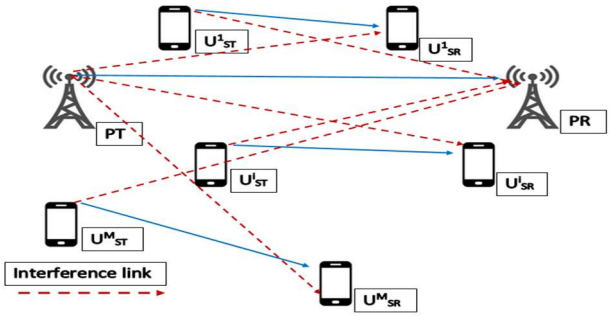

Figure. 2: Data transmitting

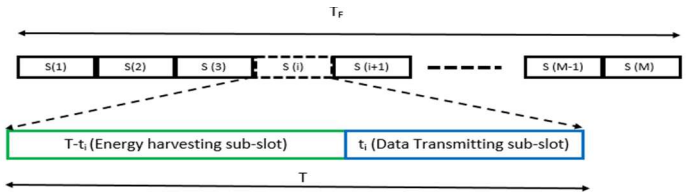

Figure. 3: Time slot structure

3.1. Notations

Various notations are employed in this work. Thus, for easier readability, a checklist of the useful notations employed in this manuscript is presented in Table 1.

3.2. Energy Harvesting

The PT from the primary network transmits constantly and provides a dedicated source of RF energy harvesting opportunity for the CRNRF-EN nodes. Each network communication duration,T, slot starts with the U_{ST}^i , first harvesting its energy from the PT's signal transmission, for a given time duration of $T - t_i$. The energy harvested

By U_{ST}^i during the energy harvesting time $T - t_i$ is E_i. Hence, E_i is defined in Equation 1, as:

$$E_i = (T - t_i)\varepsilon_i P_{PT} a_{PT,ST}^i \quad (1)$$

The P_{PT} indicates the transmission power of the primary user PT, $a_{PT,ST}^i$is the channel gain between the PT and the U_{ST}^i , while ε_i denotes the average energy harvesting efficiency of the U_{ST}^i , which henceforth will just be simply referred to as energy harvesting efficiency in rest part of the manuscript, where $\varepsilon_i \in [0, 1]$. In our implemented harvest-store-use protocol, for simplicity, the storage time is ignored.

Table 1: Summary of important notations

Notation	Description
$R^i(t_i P_{ST}^i)$	Throughput capacity of the U^i in the $SU's$ networks
P_{ST}^i	Transmission power of the U_{ST}^i
$a_{PT,ST}^i$	Channel link gain between the PT and U_{ST}^i
$b_{PT,SR}^i$	Interference channel link gain between the PT and U_{SR}^i
$g_{ST,PR}^i$	Channel link gain between the U_{ST}^i and PT
$h_{ST,SR}^i$	Interference channel link gain between the U_{ST}^i and the U_{SR}^i
E_i	Harvested energy of the U_{ST}^i
I_p	Interference threshold of the primary networks
P_{PT}	Constant transmission power of the PT
L_o	Path loss
P_{max}	Maximum transmitting power threshold for secondary user
ε_i	Energy harvesting efficiency of the U_{ST}^i
U_{ST}^i	The i^{th} transmitter of the SU networks
U_{SR}^i	The i^{th} receiver of the SU networks
n_i	AWGN at the U_{SR}^i in the SU networks
T	Slot duration
T_F	Frame duration
t_i	Transmission time of the U_{ST}^i
ϑ_i	New intermediate variable of U^i in the $SU's$ networks
N_{0i}	Noise power at the U_{SR}^i
σ^2	Rayleigh fading gain variance
I_{SR}^i	Received noise from the PT at the i^{th} user in SU networks
Γ^i	Signal to interference plus noise ratio at the i^{th} user in the SU networks
x_p	Transmitted base-band signal of PU
x_i	Transmitted base-band signals of U_{ST}^i

3.3. Data Transmitting

In the CRN-RF-EN, each U_{ST}^i starts the transmission of its data or information to U_{SR}^i, after its energy harvesting time. During the data transmission time, the transmission of U_{ST}^i to U_{SR}^i causes some interference to the PR in the primary user networks. Similarly, the transmission of PT to PR causes some interference to U_{SR}^i in the secondary user networks. However, the primary user network can allow the transmission activities as long the accumulative interference of all U_{ST}^i does not exceed the interference threshold limit of the primary user. The message received, m_i at the U_{SR}^i during the t_i transmission time is denoted in Equation 2;

$$m_i = \sqrt{P_{PT}} a_{PT,SR}^i x_p + \sqrt{P_{ST}^i} h_{ST,SR}^i x_i + n_i, \forall i \quad (2)$$

where the transmission powers of PT and U_{ST}^i are given as P_{PT} and P_{ST}^i, respectively. The $a_{PT,SR}^i$ denote the interference between PT and U_{SR}^i. The information or data channel link gain from U_{ST}^i to U_{SR}^i is denoted by $h_{ST,SR}^i$. The base-band signals originating from the PT and U_{ST}^i are represented by x_p and x_i, respectively, while the additive white Gaussian noise (AWGN) at U_{SR}^i is denoted as n_i.

4. A MATHEMATICAL MODEL

In this section, we present the mathematical model for the worst-case user capacity optimization problem for the CRN-RF-EH. The goal of the study is to optimize the throughput of the worst-case users' capacities in the CRN-RF-EH by optimally allocating jointly the transmission time and transmission power in the CRN-RF-EH, under various peculiar constraints that are associated with the CRNRF-EH.

4.1. Achievable Channel Capacity Analysis

The maximum achievable throughput of U^i is negatively impacted by the continuous signal transmission of the PT. Thus, due to this continuous transmission of PT, U_{SR}^i experiences constant interference from thePT. The received interference I_{SR}^i of the U_{SR}^i during the data transmission slot of the CRN-RF-EH is expressed in Equation 3:

$$I_{SR}^i = P_{PT} a_{PT,SR}^i, \forall i \quad (3)$$

The maximum achievable throughput of each user in the CRNRF-EH during the data transmission time or the maximum transmission rate $R^i(t_i, P_{ST}^i)$ of the i^{th} user with the transmission power P_{ST}^i and transmission time, t_i can be calculated using Equations 4-6:

$$R^i(t_i, P_{ST}^i) = t_i \, log_2\left(1 + \frac{P_{ST}^i h_{ST,SR}^i}{P_{PT} a_{PT,SR}^i + N_{0i}}\right), \forall i \quad (5)$$

$$R^i(t_i, P_{ST}^i) = t_i \log_2(1 + \Gamma^i), \forall i \quad (6)$$

where Γ^i is the signal-to-interference plus noise ratio (SINR) at the U_{SR}^i. The N0i denotes the noise power at the U_{SR}^i. The AWGN has a power spectra density (PSD) that is flat over all frequencies.

4.2. Assumptions

Some important assumptions were made in this manuscript. The channel reciprocity assumption was employed. It is assumed that the channel links experience an independent quasi-static block fading channel, this implies that the channel remains static or unchanged in one time slot, but can change in the next time slot. To achieve the upper performance limit for our numerical simulations, we assume that the channel state information (CSI) is perfectly known within the CRNRF-EH. For simplicity, the complete network slot duration time,T is normalized to 1. Without loss of generality, it is assumed that the AWGN power at all SUs is the same, i:e $N_{01} = N_{02} = N_{03} = \cdots = N_{0i} = \cdots = N_{0M-1} = N_{0M}$. While for practical network implementations, the energy harvested stored in supercapacitors to power data transmission, however the harvested energy will not always necessarily be totally used up all the time, meanwhile such restriction or non-total harvested energy consumption condition can be relaxed for network simulation for modelling for simplicity, hence in this work it is assumed that harvested energy is completely used up after data transmission. Therefore, there is no residual or left over energy at the beginning of a new energy harvesting time slot. Thus, the harvested energy during the harvesting time slot is consumed before the beginning of another harvesting time slot.

4.3. Constraint Definitions

In the CRN-RF-EH, the energy consumption of the U_{ST}^i node is highly constrained or limited to its harvested energy, E_i. thus this results in the well-known energy causality constraint of all RR-EH networks. In underlay spectrum access architecture, the cognitive transmitter node U_{ST}^i causes a certain level of interference to the PR in the primary user network. To protect PT from possible harmful interference from U_{ST}^i in the CRN-RF-EH, the minimum acceptable interference threshold by the primary user network must be enforced on the CRN-RF-EH. Thus, the allocated transmission power of U_{ST}^i in the CRN-RF-EH networks need not exceed the networks' set maximum threshold of the CRN-RF-EH. Similarly, the transmission time of the U_{ST}^i must not exceed the total communication slot duration of the CRN-RF-EH. These constraints are vital for the CRN-RF-EH and are mathematically formulated below.

4.3.1 Primary network interference constraint, C1

For the nodes in CRN-RF-EH to carry out communication on the primary user's network spectrum, the communication activities of the primary users must not be noticeably hampered by the interference from the transmission activities of U_{ST}^{i} in CRN-RF-EH. The primary user network will not tolerate any harmful interference above its maximum acceptable interference threshold,I_P, from the CRNRF-EH nodes. Therefore, the total $SU's$ interference from each communication duration slot of CRN-RF-EH must not exceed the maximum acceptable interference threshold,I_P, of the primary receiver. This is model in Equation 7:

$$g_{ST,PR}^{i} P_{ST}^{i} \leq I_P, \forall i \tag{7}$$

4.3.2 Transmission power constraint, C2

Another way the interference from CRN-RF-EH transmitting nodes is controlled is by enforcing a transmission power constraint on each U_{ST}^{i}. This helps limit the amount of interference power that gets to the PR of the primary user network from the CRN-RF-EH transmitting nodes.

Secondly, the transmitting U_{ST}^{i} should not be able to transmit at infinite power, no matter how short its allocated transmission time is. Thus, the transmission power assigned to each U_{ST}^{i} needs to be capped to the network acceptable maximum, P_{max}. This process is captured and addressed with the Constraint $C2$ as defined in Equation 8, as;

$$P_{ST}^{i} \leq P_{max}, \forall i \tag{8}$$

4.3.3 Energy causality constraint, C3

The energy consumed by U_{ST}^{i} is solely limited by how much of harvested energy E_i, that it can harvest during its energy harvesting time slot, $T - t_i$. Thus U_{ST}^{i} energy consumption during its transmission time slot t_i can not exceed the amount of energy harvested during its energy harvesting time slot $T - t_i$. Hence, this is an energy causality constraint. The energy causality constraint is expressed in Equation 9 and Equation 10, as:

$$P_{ST}^{i} \leq n_i (T - t_i)\, e_{PT,ST}^{i} P_{PT}, \forall i, \tag{9}$$

$$P_{ST}^{i} t_i \leq E_i, \forall i. \tag{10}$$

4.3.4 Transmission time constraint, C4

In the CRN-RF-EH framework, the U_{ST}^{i}, if the U_{ST}^{i} used all the entire communication slot duration T, to harvest energy, that is $T - t_i = T, (t_i = 0)$, thus U_{ST}^{i} will not be able to transmit its data or information, hence $t_i \neq 0$. Also, given that the CRN-RF-EH implements the harvestand-then-transmit protocol, thus U_{ST}^{i} can not harvest energy using its entire slot duration. Similarly, it is not possible to allocate the entire T to t_i as its transmission time, as there will be no prior harvested energy for the U_{ST}^{i} to transmit with. Hence must be $t_i \neq T$. These conditions are implemented by Constraint $C4$ as depicted in Equation 11;

$$0 < t_i < T, \forall i. \tag{11}$$

5. THROUGHPUT FAIRNESS RESOURCE ALLOCATION

In energy harvesting network, harvested energy utilization and resource allocation starvation or unfairness are of great concern. Hence, the goal here is to optimize the worst-case user capacity of the CRN-RF-EH.

5.1. Problem Formulation: Max-min

In wireless communication and network resource allocation, fairness metrics play a crucial role in balancing efficiency and user satisfaction. Among the widely used fairness metrics are proportional fairness, geometric mean fairness and max-min fairness. While max-min fairness ensures that the most disadvantaged users or weaker users get priority before increasing others resource allocation, in contrast proportional fairness and geometric mean fairness can lead to resource starvation for weaker users, thus only max-min fairness metric in considered in this paper. We propose a resource allocation fairness scheme, using the max-min maximization framework while jointly optimizing the transmission and transmit power of the U_{ST}^{i}. The throughput capacity $R^i(t_i, P_{ST}^{i})$ of the underlay CRN-RF-EH is dependent on transmission time, $\boldsymbol{t}$ and transmission power, $\boldsymbol{P}$ vectors. The allocated transmission time and power are defined as:$t = [t_1, t_2, t_3, \cdots, t_i, \cdots, t_{M-1}, t_M]$ and $P = [P_{ST}^{1}, P_{ST}^{2}, P_{ST}^{3}, \cdots P_{ST}^{i}, \cdots, P_{ST}^{M-1}, P_{ST}^{M}]$, respectively. The optimization problem OP1 to maximize $R_i(t_i, P_{ST}^{i})$ is formulated in Equation 12 as;

$$OP1: \max_{t,P} \min_{i \in M} R^i(t_i, P_{ST}^{i})$$

$$s.t.:$$

$$C1: g_{ST,PR}^{i} P_{ST}^{i} \leq I_p, \forall i$$

$$C2: P_{ST}^{i} \leq P_{max}, \forall i$$

$$C3: P_{ST}^{i} t_i \leq E_i, \forall i$$

$$C4: 0 < t_i < T, \forall i$$

$$C5: P_{ST}^{i}, t_i > 0, \forall i \tag{12}$$

The Constraint $C5$ ensures that t_i and P_{ST}^{i} are non-negative values. Given that a convex optimization problem formation is much efficient and easy to solve with various optimization techniques, however, the formulated optimization problem $OP1$ is a non-convex optimization problem. This is due to the max-min formulation and coupling of the optimization variables in the objective function and the constraint $C3$. Thus the $OP1$ need to be transformed to its equivalent convex optimization problem such that a global optimal solution can be obtained.

5.2. Problem Formulation: Worst-case user Capacity Maximization

Since $R^i(t, P)$is an ascending function with regard to both t and, P and is a multivariate objective function, problem $OP1$ can be restated into its epigraph form. To do this we introduce a slack variable Ω, where $\Omega \triangleq \min_{i \in M} R^i(t_i, P_{ST}^{i})$. This transforms the multivariate objective function into a linear function. Therefore, since linear functions are convex, thus the objective function is a convex objective function (Boyd, S., & Vandenberghe, L. 2004). Thus, $OP2$ is formulated in Equation 13, as:

$$OP2: \max_{t,P,\Omega} \Omega$$

$$s.t.:$$

$$C1': \Omega - R^i(t_i, P_{ST}^{i}) \leq 0, \forall i$$

$$C2': g_{ST,PR}^{i} P_{ST}^{i} \leq I_p, \forall i$$

$$C3': P_{ST}^{i} \leq P_{max}, \forall i$$

$$C4': P_{ST}^{i} t_i \leq E_i, \forall i$$

$$C5': 0 < t_i < T, \forall i$$

$$C6': P_{ST}^{i}, t_i > 0, \forall i \tag{13}$$

Note that the objective function of the previous problem, $OP1$ is equivalent to maximizing over the slack variable Ω of $OP2$, such that $\min_{i \in M} R^i(t_i, P_{ST}^{i}) \geq \Omega, \forall i$. Consequently, all user achievable rates

have a lower bound represented by the slack variable Ω . In this case, Ω represents the lowest user rate utility that can be achieved for every user, and it is optimized to provide every user, irrespective of their channel or cell-edge user conditions, a consistently good utility level of service.

Notice that there is non-convexity of both constraints $C1'$ and $C4'$ arises from the coupled variables, i.e.,t_i and P_{ST}^i. To address this challenge of transforming $OP2$ to a standard convex optimization problem $OP3$, we introduce the use of an intermediate variableχ. Let $\chi_i = P_{ST}^i t_i, i = 1,2,3,\cdots,M-1,M$. Thus, $OP3$ is formulated in Equation 14, as:

$$OP3: \max_{t,\chi_i,\Omega} \Omega$$

$$s.t.:$$

$$C1'': \Omega - R^i\left(t_i, \frac{\chi_i}{t_i}\right) \leq 0, \forall i$$

$$C2'': \chi_i g_{ST,PR}^i \leq I_p t_i, \forall i$$

$$C3'': \chi_i \leq P_{max}\, t_i, \forall i$$

$$C4'': \chi_i \leq E_i, \forall i$$

$$C5'': 0 < t_i < T, \forall i$$

$$C6'': \chi_i, t_i > 0, \forall i \qquad (14)$$

where $\chi = [\chi_1, \chi_2, \chi_3, \cdots, \chi_i, \cdots, \chi_{M-1}, \chi_M]$is the vector of the new optimization variable. Proposition 1: The optimization problem $OP3$ is convex. For proof of convexity of $OP3$ see Appendix A.

Since the optimization problem, $OP3$ is a standard convex optimization problem w.r.t energy and time allocations, the $OP3$ can be solved by standard convex optimization techniques. Recently, several efficient solvers have been used to solve standard convex optimization formulation for resource allocation problems in energy-harvesting cognitive radio networks (Wang et al., 2020). In science and engineering, optimization software solvers are potent toolkits that are used to simulate and solve optimization programming problems (Koch et al., 2022). Several widely used commercially licensed optimization software solvers are the CPLEX (Lahsen-Cherif et al., 2021), CONOPT (Nojavan et al., 2023), YALMIP (Li et al., 2021) and GUROBI (Liu et al., 2024); they can be found in the literature. Various wireless communication networks' optimization problem formulations have been solved using optimization software solvers (Lahsen-Cherif et al., 2021). The CONOPT solver is a robust that can solve large real-time network systems. The performance CONOPT solver on large network system is evaluated on IEEE 33-bus and IEEE 69-bus test systems for conducting load flow calculations in radial distribution networks. The CONOPT solver outputs are accurate and fast in their convergence to global solutions in standard test systems (Rakočević et al., 2024). The CONOPT solver is used to solve the optimization problem $OP3$. The CONOPT is an optimization solver tool that is based on the generalized reduced-gradient (GRG) algorithm for solving large-scale non-linear optimization problems (Andrei, 2017). The CONOPT assumes all variables are continuous and all constraints are smooth with smooth first derivatives. The CONOPT solver does not handle **integer** or **binary** decision variables well, making it unsuitable for mixed-integer nonlinear programming (MINLP) without additional techniques. CONOPT solver requires that a feasible starting point be provide while poor initial guesses or starting point can lead to slow convergence, while if variables and constraints are not properly scaled, CONOPT solver may experience numerical instabilities. It is available as a Fortran Subroutine library. The CONOPT is implemented in MATLAB/TOMLAB software environment. The GRG algorithm is given in Algorithm 1.

Algorithm 1: The generalized reduced gradient (GRG) Algorithm.

Given the objective function,$f(x)$ equality constraints$g_i(x)$, and inequality constraints$h_i(x)$, x is the set of decision variables and X is the feasible domain, where x is in the feasible domain or $x \in X$.

Step 1: Initialize and start the algorithm:

Choose an initial feasible point for the set of the decision variables as $x(0)$, where $x(0)$ satisfies the equality constraints, $g_i(x) = 0$ and the inequality constraints, $h_i(x) \leq 0$.

Initialize termination parameter, φ $(\rightarrow 0^+)$

Initialize the iteration counter $m = 0$

Step 2: Relax the inequality constraints and define the basic and non-basis variables:

Relax the inequality constraints by introducing slack variables

Partition the set of variables x into basic variable x_B and non-basic variables x_N .

Step 3: Compute the Jacobian:

Compute the Jacobian of $g(x)$ with respect to the basic variables, x_B:

$$J_B = \frac{\partial g(x)}{\partial x_B}.$$

Compute the Jacobian of g(x) with respect to the non-basis variables, x_N:

$$J_N = \frac{\partial g(x)}{\partial x_N}.$$

Step 4: Compute the reduced gradient:

Calculate the reduce gradient of the objective function:

$$\nabla f(x) = \left[\frac{\partial f}{x_1}, \frac{\partial f}{x_2}, \frac{\partial f}{x_3}, \ldots, \frac{\partial f}{x_k}\right].$$

Partition the reduced gradient of the objective function into the basic and non-basic reduced objective functions, as:

$$\nabla f(x) = \begin{pmatrix} \nabla f_B(x) \\ \nabla f_N(x) \end{pmatrix}$$

Recomputed the reduced gradient of the objective function as:

$$\nabla f_R(x) = \nabla f_N(x) - \nabla f_B(x)(J_B^{-1} J_N)$$

Step 5: Compute the 2-norm and check for termination:

If $\|\nabla f_R(x(m))\| < \varphi$

Then $x_{optimum} = x(m)$

Else update the search direction vector d for the non-basic and basic variables, as:

$$d_N = -\nabla f_R(x)$$

and

$$d_B = -(J_B^{-1} J_N) d_N$$

Step 6: Determine the step size, $\alpha^{(m)}$:

Perform a line search to find the step size$\alpha^{(m)}$, which sufficiently reduces the objective function, such that $f(x(m) + \alpha^{(m)} d)$ is minimum, while maintaining the feasibility with respect to the constraints.

Update variables

$$x_B(m+1) = x_B(m) + \alpha^{(m)} d_B$$

$$x_N(m+1) = x_N(m) + \alpha^{(m)} d_N$$

Step 7: Update iteration counter:

Set $x(m+1) = (x_B(m+1), x_N(m+1))$

Increment the iteration counter as, $m = m + 1$;

if $\|\nabla f_R(x(m+1)\| < \varphi$

input $x_{optimum} = x(m+1)$

Else

Go to Step 3:

Step 8: End algorithm.

6. NUMERICAL RESULTS AND DISCUSSIONS

In this section, the JOTPA resource allocation scheme performance evaluations for CRN-RF-EH worst-case user capacity maximization are investigated through numerical simulations and the results are presented. Since the goal of this paper is to explore

the worst-case user capacity maximization for the CRN-RF-EH, w.r.t. the SUs' energy causality constraints, primary user interference threshold limit, communication slot duration, and maximum transmission power threshold, the CONOPT solver is employed to solve the $OP3$. The CONOPT is a robust commercial optimization tool that can solve highly dense nonlinear optimization problems efficiently. In our simulations, a CRN-RF-EH which consists of three SU users, $(M = 3)$ in the SU network and one PT and PR in the PU network are considered. The SU network exists in a square area bounded by(0,0) ,(0,0) and (10,10). The U_{ST}^{i} is fixed at (1,9), (9,2) and (8,8). The U_{SR}^{i} is randomly distributed. The average distance of the primary network's transmitter and receiver from the $SU's$ networks are set to 15m and 20m, respectively. Except otherwise stated, other CRN-RF-EH parameters are assigned as follows. The duration of slot T T is normalized to 1 unit. The maximum interference threshold for the primary receiver is $I_p = 1W$. The PT constant transmission power $P_{PT} = 15W$, energy harvesting efficiency $\varepsilon_i = 0.6$ and Maximum transmitting power threshold for secondary user, $P_{max} = 3W$.

The channel power gains are modeled as $a_{PT,ST}^{i} = a_{PT,ST}^{i'} d_{PT,ST}^{-\alpha}$, $b_{PT,SR}^{i} = b_{PT,SR}^{i'} d_{PT,SR}^{-\alpha}$, $h_{ST,SR}^{i} = h_{ST,SR}^{i'} d_{ST,SR}^{-\alpha}$, and $g_{ST,PR}^{i} = g_{ST,PR}^{i'} d_{ST,PR}^{-\alpha}$. The Rayleigh fading terms are denoted as;$a_{PT,ST}^{i'}$, $b_{PT,SR}^{i'}$, $h_{ST,SR}^{i'}$ and $g_{ST,PR}^{i'}$. The Rayleigh fading terms are independent exponential random variables. The distances between thePT and ST, and between PT and SR, and between ST and SRS and between ST and PR are denoted by $d_{PT,ST}$, $d_{PT,SR}$, $d_{ST,SR}$, and $d_{ST,PR}$, respectively. α denotes the path-loss exponent and is set to 3.7, for urban cellular environment. All the channel links experience a combination of Rayleigh fading and path loss. The distance-dependent path loss is considered as the large-scale fading. The Rayleigh fading is considered to be the small-scale fading (Kaur et al., 2017). The bandwidth, B is set to 1MHz. Numerical simulations are repeated over 1, 000 different random fading channel realizations and the results are averaged. The proposed JOTPA scheme is compared with the BRTOPA scheme. The BRTOPA allocates transmission time based on a biased-randomized Gaussian probability distribution.

6.1. Effect of Duration Slot

Figure. 4 presents the investigation of the response of worst-case user capacity to relative variation of slot duration in CRN-RF-EH. Figure. 4 shows the worst-case user capacity performance in the CRN-RF-EN across the resource allocation schemes for increasing slot duration simulations. Generally, it is observed that in the worst-case user capacity improves when the slot duration is increased for the investigated resource allocation schemes.

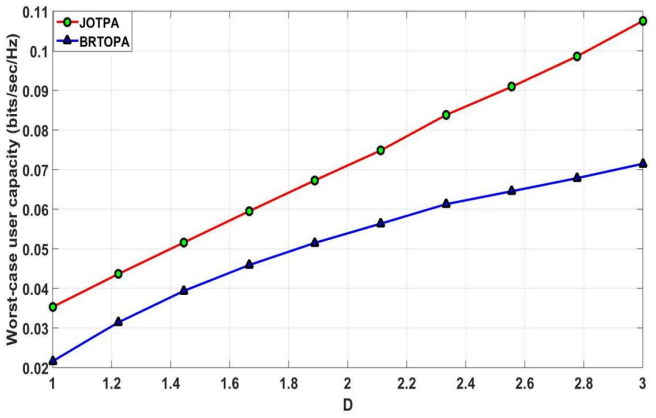

Figure. 4: Effect of relative slot duration length

The fact behind this observation is that in the CRN-RF-EH, a lengthened slot duration provides more time for both the energy harvesting phase and signal transmission phase for the SUs to harvest energy from the primary user network and transmit their data, respectively. However, JOTPA outperformed the BROTPA scheme at any given slot duration. In Figure. 4, the performance results indicate that the JOTPA scheme over BROTPA is significantly more improved at relatively higher slot duration than lower slot duration. The JOPPA leverages the relatively increased slot duration in the CRN-RF-EH to produce better-optimized network performance solutions. The JOTPA scheme offers an average performance gain of about 28.2% over the BRTOPA scheme.

6.2. Effect of the Distance of Primary user Transmitter

In the CRN-RF-EH, Figure.5 demonstrates the impact of the variation of the PU transmitter distance to the SU networks on the worst-case user capacity performance. As seen from Figure.5, generally for the presented resource allocation schemes, the throughput capacity of the CRN-RF-EN distances inversely with increasing average distance of the primary user's transmitter distance for the $SU's$ network. This is due to the established experimental evidence that the received signal strength (RSS) at the receiver decreases inversely as the distance between the transmitter and the receiver increases. Hence in the energy harvesting phase, the amount of harvested energy by the RF energy harvesting cognitive nodes and subsequently the transmitting signal power available to

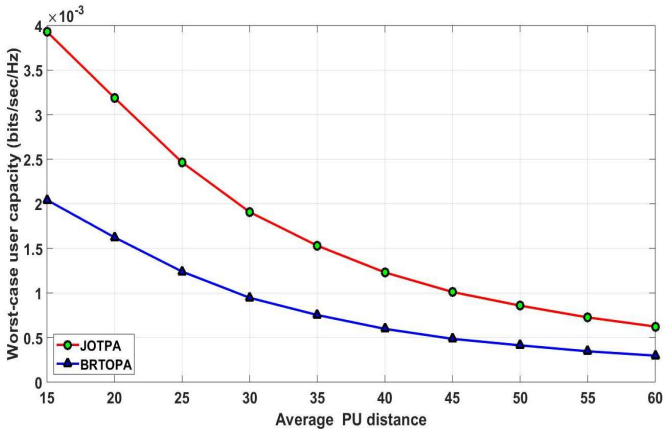

Figure. 5: Effect of average PU transmitter distance on SU worst-case user capacity

The cognitive radio node in the transmission phase will inversely decrease. However, in comparison, it is evident that when considering the throughput attained using the max-min fairness criterion, the suggested JOTPA system consistently performs better than the BRTOPA scheme. The JOTPA offers more flexibility in resource utilization by jointly optimizing the transmission time and transmission power to adapt optimally with the increasing average $PU's$ transmitter distance. In Figure.5, JOPTA achieves an average performance gain of about 50.8% over the BRTOPA scheme.

6.3. Effect of Secondary user Transmission Power Threshold

The performance study of the impact of varying SUs' transmission power threshold P_{max} on the worst-case user capacity in CRN-RFEH network power consumption of the CCRRN system is presented in Figure.6. The result depicts that as the SUs transmission power threshold rises, the worst-case user capacity performance for both schemes is generally improved. The worst-case user capacity performance slope is steeper at lower SU transmission power thresholds, while its performance slope is less steep at higher SU transmission power thresholds. These observations follow the logarithm law, supported by the Shannon channel capacity law. Furthermore, for a higher SU transmission power threshold, as the SU increases its transmit power under a set PU network interference temperature limit in the underlay spectrum access mode, the SU interference received at the PU networks will start to increase. If this situation is not checked by the SUs' networks, this can create a possible scenario where

$SU's$ network violates the interference threshold of the primary network. Thus to avoid this scenario, the CRN-RF-EH network starts capping the SUs' transmission power, consequently, as a result, the worst-case user capacity tends towards being compressed or saturated by the CRN-RF-EH. The performance evaluation result shows in Figure.6 depicts that JOPTA delivers an average performance enhancement of 45.6% above BROTPA.

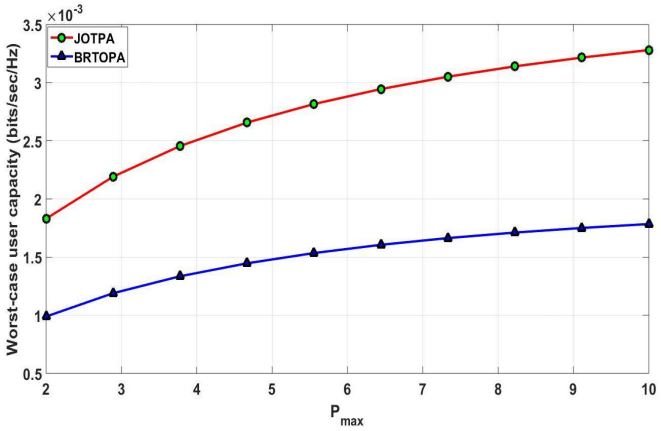

Figure. 6: Effect of SU transmission power threshold

6.4. Effect of Path-loss Exponent

In Figure.7, the performance study of the response of worst-case user capacity to path loss exponent variation. As the path loss exponent increases, the worst-case user capacity decreases, this can be due to absorption and reflection losses due to urban buildings and structures, mountains etc., in the radio propagation environment. As the path loss exponent increases, the attenuation of transmitted power from the primary user transmitter towards the CRN-RF-EH increases. This leads to low harvested RF energy at the source node in the CRN-RF-EH.

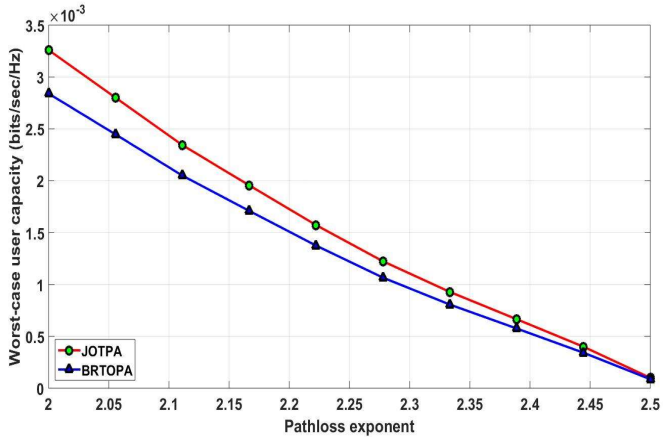

Figure.7: Effect of path loss exponent

Subsequently, in the CRN-RF-EH, the transmission of the source node to the destination node in an increasing path loss exponent environment result in a low received signal-to-noise ratio (SNR) at the destination node. Thus, the throughput capacity at the destination node decreases. This supports the Shannon channel capacity theory. Thus Figure 7 illustrates how the path loss exponent variable indirectly affects the worst-case user capacity. The result shows that at a lower path loss exponent value, the JOTPA scheme performed significantly better than the BRTOPA scheme, however, the performance advantage of JOTPA scheme over the BRTOPA scheme starts to drop or decline as approaches that of BRTOPA as the path loss exponent increases. In all, a 13.0% average performance improvement of the JOTPA scheme over the BRTOPA is observed in Figure.7.

6.5. Effect of Primary user Transmission Power

The CRN-RF-EH performance study for the effect of varying primary user transmission power on the worst-case user capacity is presented in Figure.8. From the result, as the primary user increases its transmission power, the worst-case user capacity simultaneously increases. This indicates that the higher the primary user transmission power, the more energy that can be harvested by the SUs. This indicates that as the transmission power of PU in the primary user network increases, the energy harvested by the SUs in secondary user networks, in the energy harvesting epoch also increases. With more energy available for the SUs, there is a higher power capacity for achieving increased data transmission rates during the SUs' data transmission phase. Consequently, this leads to an improved worst-case user capacity in the CRN-RF-EH. The simulation results demonstrate that the JOTPA resource allocation scheme performs better than the baseline resource scheme of BRTOPA. The comparative result in Figure.8 indicates that the worst-case user capacity performance gap between JOTPA and BRTOPA widens as the primary user transmission power increases. The performance of JOTPA over BRTOPA increases at higher primary user transmission power levels. On the average, JOTPA provides a performance improvement of 47.9% over BRTOPA.

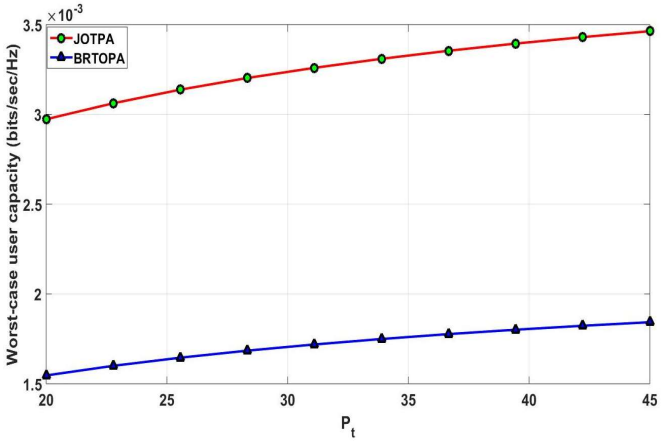

Figure. 8: Effect of primary user transmission power

7. Conclusion

In this paper, we have studied the network resource allocation fairness optimization problem for CRN-RF-EH to ensure that the throughput is fairly allocated to each user in the CRN-RF-EH system. To achieve this goal, we formulated a max-min resource allocation optimization problem. The formulated resource allocation problem is observed to be a non-convex optimization problem. We transformed the formulated non-convex problem into a resource allocation convex optimization problem by introducing a series of auxiliary variables. We proved that the transformed resource allocation optimization problem is concave. We maximize the CRN-RF-EH worst-case user throughput capacity through the proposed JOTPA scheme under the prevailing CRN-RF-EH constraints. Our analysis showed that when the CRN-RF-EH's U_{ST}^{i} uses up all of the harvested RF energy, the worst-case user throughput capacity maximization is reached. Through simulation results, we have shown that our proposed solution always achieves the superior performance compared with the conventional BRTOPA scheme. The analysis into the network system radio resource allocation fairness performances of the CRN-RF-EH in this paper is based on the assumption of perfect CSI

among all users, consequently, it will be interesting for future work direction to characterize the effect of the uncertainty due to imperfect CSI among all users in the CRN-RF-EH. While our proposed scheme guaranteed fairness to worst-case users in the network, however our proposed scheme cannot guarantee fairness for worst-case users in the networks with prioritized users or minimum rate requirement users.

CONFLICT OF INTEREST:

The authors declare no conflicts of interest.

REFERENCES

Andrei, N. (2017) "Continuous nonlinear optimization for engineering applications in GAMS technology" *Springer Optimization and Its Applications,* ISBN 978–1–4614-6796-0. https://doi.org/10.1007/978-1-4614 -6797-7.

Biswas, S., Dey, S., and Shirazinia, A. (2019) "Sum throughput maximization in a cognitive multiple access channel with cooperative spectrum sensing and energy harvesting," *IEEE Transactions on Cognitive Communications and Networking*, Volume 5, Issue 2, pp. 382–399, https://doi.org/10.1109/TCCN.2019.2908860.

Boyd, S., and Vandenberghe, L. (2004). "Convex optimization" *Cambridge University Press.*

Cheng, Y., Fu, P., Ding, Y., Li, B., and Yuan, X. (2017) "Proportional fairness in cognitive wireless powered communication networks," *IEEE Communications Letters*, Volume 21, Issue 6, pp. 1397–1400, https://doi.org/10.1109/LCOMM.2017.2675904

Gholikhani, M., Roshani, H., Dessouky, S., and Papagiannakis, A. T. (2020) "A critical review of roadway energy harvesting technologies," *Applied Energy*, Volume 261, p. 114388, https://doi.org/10.1016/j.apenergy.2019.114388.

Hu, Z., Zhou, F., Zhang, Z., and Zhang, H. (2017) "Optimal max-min fairness energy harvesting resource allocation in wideband cognitive radio network,"*IEEE Vehicular Technology Conference (VTC Spring)*, pp. 1–5, https://doi.org/10.1109/VTCSpring.2017.8108631.

Jiang, F., Yi, W., Li, S., Zhu, B., and Yu, W. (2017) "Joint optimization of spectrum sensing and energy harvesting for cognitive radio network," *IEEE International Symposium on Parallel and Distributed Processing with Applications and IEEE International Conference on Ubiquitous Computing and Communications (ISPA/IUCC),* pp. 423–427, https://doi.org/10.1109/ISPA/IUCC.2017.00068.

Kalamkar, S. S., Jeyaraj, J. P., Banerjee, A., and Rajawat, K. (2016) "Resource allocation and fairness in wireless powered cooperative cognitive radio networks," *IEEE Transactions on Communications*, Volume 64, Issue 8, pp. 3246–3261, https://doi.org/10.1109/TCOMM.2016.2581162.

Koch, T., Berthold, T., Pedersen, J., and Vanaret, C. (2022) "Progress in mathematical programming solvers from 2001 to 2020," *EURO Journal on Computational Optimization*, Volume 10, https://doi.org/10.1016/j.ejco.2022.100031.

Kaur, T., Singh, J., and Sharma, A. (2017) "Simulative analysis of Rayleigh and Rician fading channel model and its mitigation," *International Conference on Computing, Communication and Networking Technologies (ICCCNT)*, pp.1–6, https://doi.org/10.1109/ICCCNT.2017.8204186.

Lee, B., and Shin, W. (2023), "Max-min fairness precoder design for rate-splitting multiple access: Impact of imperfect channel knowledge," *IEEE Transactions on Vehicular Technology*, Volume 72, Issue 1, pp. 1355–1359, https://doi.org/10.1109/TVT.2022.3206808.

Li, Y., Ren, X., Wang, S., Han, Y., and Zhang, T. (2021) "Target detection with optimal power allocation and quantization for distributed MIMO DFRC system," *CIE International Conference on Radar (Radar)*, pp. 2559–2563, https://doi.org/10.1109/Radar53847.2021.10028539.

Liu, M., and Zhang, L. (2020), "Resource allocation for d2d underlay communications with proportional fairness using iterative-based approach," *IEEE Access*, Volume 8, pp. 143 787–143 801, https://doi.org/10.1109/ACCESS.2020.3010091.

Liu, S., Wang, D. Z. W., Tian, Q., and Lin, Y. H. (2024) "Optimal configuration of dynamic wireless charging facilities considering electric vehicle battery capacity," *Transportation Research Part E: Logistics and Transportation Review*, Volume 181, p. 103376, https://doi .org/10.1016/j.tre.2023.103376.

Nojavan, S., and Attar, A. (2023) "Optimal energy operation in dc microgrids including hydro-pumped storage in the presence demand response program," *International Conference on Technology and Energy Management (ICTEM)*, pp.1–5, https://doi.org/10.1109/ICTEM56862.2023.10083898.

Raeisi-Varzaneh, M., Dakkak, O., Habbal, A., and Kim, B. S. (2023) "Resource scheduling in edge computing: Architecture, taxonomy, open issues and future research directions," *IEEE Access*, Volume 11, pp.25329–25350, https://doi.org/10.1109/ACCESS.2023.32 56522.

Rakočević, S., Ćalasan, M., Mujović, S., Milovanović, M., and Aleem, S. A. (2024) "Efficient CONOPT Solver for Load Flow Calculations in Modern Radial Distribution Systems" *Arabian Journal for Science and Engineering*, Volume 49, Issue 12, pp: 15985-16003, https://doi.org/10.1007/s13369-024-08802-3.

Sharma, P., and Singh, A. K. (2023) "A survey on rf energy harvesting techniques for lifetime enhancement of wireless sensor networks," *Sustainable Computing: Informatics and Systems*, Volume 37, p. 100836, https://doi.org/10.1016/j.suscom.2022.100836.

Shi, H., Prasad, R.V., Onur, E., and Niemegeers, I.G. (2014) "Fairness in wireless networks: issues, measures and challenges,"*IEEE Communications Surveys & Tutorials*, Volume 16, Issue 1, pp. 5–24, https://doi.org/10.1109/SURV.2013.050113.00015.

Singh, A., Bhatnagar, M. R., and Mallik, R. K. (2020), "Secrecy outage performance of SWIPT cognitive radio network with imperfect CSI," *IEEE Access*, Volume 8, pp. 3911–3919, https://doi.org/10.1109/ACCESS.2019.2962382.

Tran, H., Akerberg, J., Bjorkman, M., and Ha-Vu, T., (2019), "RF energy harvesting: an analysis of wireless sensor networks for reliable communication," *Wireless Networks*, Volume 25, Issue 1, pp. 185–199, https://doi.org/10.1007/s11276-017-1546-6.

Wang, E. Z., and Lee, C. C. (2022) "The impact of information communica -tion technology on energy demand: Some international evidence," *International Review of Economics & Finance*, Volume 81, pp. 128–146, https://doi.org/10.1016/j.iref.2022.05.008.

Wang, T., Hu, F., Cao, F., Mao, Z., and Ling, Z. (2020) "Sum-throughput maximization based on the significance and fairness of sensors for energy and information transfer in virtual MIMO-WBAN," *IEEE Transactions on Vehicular Technology*, Volume 69, Issue 11, pp. 13 400–13 409, https://doi.org/10.1109/TVT.2020.3025915.

Wu, Q., Guan, X., and Zhang, R. (2022) "Intelligent reflecting surface-aided wireless energy and information transmission: An overview," *Proceedings of the IEEE*, Volume 110, Issue 1, pp. 150–170, https://doi.org/10.1109/JPROC.2021.3121790.

Xu, D., and Li, Q. (2018) "Energy efficient joint channel and power allocation for energy harvesting cognitive radio networks," *IEEE International Symposium on Dynamic Spectrum Access Networks (DySPAN)*, pp. 1–5, https://doi.org/10.1109/DySPAN.2018.8610488.

Zakariya, A. Y., Tayel, A. F., Rabia, S. I., and Mansour, A. (2020) "Modeling and analysis of cognitive radio networks with different channel access capabilities of secondary users," *Simulation Modelling Practice and Theory*, Volume 103, p. 102096, https://doi.org/10.1016/j.simpat.2020.102096.

Zhang, Z., Pang, H., Georgiadis, A., and Cecati, C. (2019) "Wireless power transfer—an overview," *IEEE Transactions on Industrial Electronics*, Volume. 66, Issue 2, pp.1044-1058, https://doi.org/10.1109/TIE.2018.2835378.

APPENDIX A

Proof of Proposition 1:

Since the objective function of OP*3* is an epigraph linear function or an affine function in Ω hence the objective function is a linear function $\mathbb{R}^n$ of the form

$$f(\Omega) = a^T\Omega + b,$$

Where n is the dimension of the input vector, a is a constant vector, Ω is the variable vector and b *is* a constant scalar. _

The Hessian matrix of $f(\Omega)$ is the matrix of second-order partial derivatives:

$$\mathrm{H} = \nabla^2 f(\Omega)$$

Since $f(\Omega)$ is linear, its first derivative is constant:

$$\nabla f(\Omega) = a$$

While the second derivative is:

$$\nabla^2 f(\Omega) = 0$$

This means the Hessian matrix of *OP3* is a zero matrix. A function is convex if its Hessian matrix is positive semidefinite, meaning all its eigenvalues are non-negative. Similarly, a function is concave if its Hessian matrix is negative semidefinite, meaning all its eigenvalues are non-positive. Hence the Hessian matrix of *OP3* both positive semidefinite and negative semidefinite.

A linear or affine function is both convex and concave because its Hessian is a zero matrix. For the constraint set of *OP3*, the Constraint $C1''$ is a Logarithmic function bounded by a linear function, Ω. Logarithmic and linear functions are both convex sets. In addition, the Constraints $C2'' - C6''$ are all linear convex constraints set. Therefore, *OP3* is a standard convex optimization problem that maximizes a concave function over convex constraints set.